Proceedings of the 7th International Symposium on Cavitation
CAV2009 – Paper No. 78
August 17-22, 2009, Ann Arbor, Michigan, USA

Numerical Investigation of Thermodynamic Effect on Unsteady Cavitation in Cascade

Yuka IGA
Institute of Fluid Science, Tohoku Univ.
Sendai, Miyagi, JAPAN

Naoya OCHIAI
Institute of Fluid Science, Tohoku Univ.
Sendai, Miyagi, JAPAN

Yoshiki YOSHIDA
Japan Aerospace Exploration Agency (JAXA)
Kakuda, Miyagi, JAPAN

Toshiaki IKOHAGI
Institute of Fluid Science, Tohoku Univ.
Sendai, Miyagi, JAPAN

ABSTRACT

In the present study, the thermodynamic effect on unsteady cavitation is investigated in cascade in water and liquid nitrogen at different freestream temperatures. Cavitation flowfield is simulated based on self-developed locally homogeneous model of a compressible gas-liquid two-phase medium, which is available to treat unsteady cavitation. For calculation of thermodynamic effect on cavitation, simplified thermodynamic model for the locally homogenous medium is used where local saturated vapor pressure changes with depending on rate of heat transfer by evaporation and condensation. In the result of the numerical analysis, the difference of cavitating flowfields is reproduced numerically in water and liquid nitrogen at different freestream temperature concerning the cavity surface profile and distribution of the evaporation region. Also the thermodynamic effect on cavitation in water and liquid nitrogen is investigated by comparing the cavity volumes. Then, well known thermodynamic effect on cryogenic cavitation can be reproduced numerically in liquid nitrogen, where development of the cavity is suppressed according to increase of freestream temperature. On the other hand, the inverse thermodynamic effect, which is experimentally observed in single hydrofoil in water, is reproduced under the condition of unsteady cavitation in water in the present study.

INTRODUCTION

Cavitation instabilities such as rotating cavitation and cavitation surge in turbopump inducer of liquid rocket are known to be affected by “thermodynamic effect”, which is easy to appear in cryogenic fluid or hot water. The thermodynamic effect is good effect for fluid machinery because when latent heat is absorbed from liquid phase with evaporation, liquid temperature decreases, saturated vapor pressure decreases, then evaporation is going to be hard to occur, it means development of cavitation will be suppressed. Generally, the effect is said to appear more prominently in higher temperature condition.

Although there are researches which are concerning the thermodynamic effect on cavitation, the effect on unsteady cavitation, especially on cavitation instabilities, has not yet been clarified because time and space distributions of temperature, phase change region and saturated pressure are hard to be obtained inside unsteady cavitation. For example, Cervone et al. [1] found inverse thermodynamic effect in experiment of single hydrofoil in water tunnel, where cavitation becomes longer and thicker according to increase of freestream temperature. They concluded the article by that the inverse thermodynamic effect may be explained by solid blockage effect caused by the tunnel wall. It can be said that unknown mechanism is remained in thermodynamic effect on unsteady cavitation, which cannot be explained by mechanism of static fluid or steady flow. Also, because water and cryogenic fluid have inverse temperature gradient of heat conduction coefficient, heat transport and heat conduction associated with unsteady flowfield are considered to be important when thermodynamic effect on cavitation will be considered.

In the previous study, the present authors have reproduced the frequency characteristics of the break-off phenomenon of sheet cavitation and have clarified two mechanisms of the break-off phenomenon in the cascade [2]. We have also reproduced three types of cavitation instabilities; super and sub synchronous rotating cavitations, and cavitation surge, which occur by different mechanisms, through numerical analysis of the three-blade cyclic cascade, without adding a model or boundary condition for individual phenomena [3]. In the study, the occurrence condition or propagation velocity ratio, which have been well documented based on experimental results, were reproduced qualitatively. In addition, the possibility of the suppression of cavitation instabilities by a jet flow through a slit on cascade blades was reported [4]. Furthermore, the numerical method was extended to be able to capture the temperature distribution in the flowfield with cavitation by adding energy conservation equation [5]. The numerical method developed by present authors is considered to be

applicable for numerical simulation of thermodynamic effect on cavitation and cavitation instabilities.

The purpose of the present study is clarification of characteristics of thermodynamic effect on unsteady cavitation. Unsteady cavitation is reproduced in three-blade flat-plate cascade with working fluid of water and liquid nitrogen. Two kinds of freestream temperatures are set for calculation of each fluid. Simplified numerical method is used for calculation of thermodynamic effect, where local saturated vapor pressure changes with depending on amount of heat transfer accompanied by evaporation and condensation. From the numerical results, thermodynamic effect in water and liquid nitrogen is investigated by comparing the cascade head performances and cavity volumes. The flowfields are analyzed in detail with particular attention given to difference of distributions of evaporation and condensation regions in each fluid or at each freestream temperature. Additionally, the inverse thermodynamic effect in unsteady cavitation in water is discussed.

NUMERICAL METHOD

Locally Homogeneous Model of a Compressible Gas-Liquid Two-phase Medium. In the present study, cavitation flowfield is simulated based on self-developed homogeneous model; locally homogeneous model of a compressible gas-liquid two-phase medium [2]. In the model, by considering a gas-liquid two-phase field as a pseudo-single phase medium, the Navier-Stokes (N-S) equations for continuum can be applied to cavitating flowfield in which there is discontinuity between gas and liquid phases. By assuming local equilibrium of pressures and temperatures between the gas and liquid phases, the governing equations for the gas-liquid medium are expressed by a simple form as following compressible gas-liquid N-S equations:

$$\frac{\partial \mathbf{Q}}{\partial t}+\frac{\partial\left(\mathbf{E}_j-\mathbf{E}v_j\right)}{\partial x}=\mathbf{S} \quad , \qquad \mathbf{Q}=\begin{pmatrix}\rho\\ \rho u_i\\ \rho Y\end{pmatrix},\ \mathbf{E}_j=\begin{pmatrix}\rho u_j\\ \rho u_i u_j+\delta_{ij}p\\ \rho u_j Y\end{pmatrix},\ \mathbf{E}v_j=\begin{pmatrix}0\\ \tau_{ij}\\ 0\end{pmatrix},\ \mathbf{S}=\begin{pmatrix}0\\ 0\\ \dot{m}\end{pmatrix}, \tag{1}$$

where ρ, p, and u are the density, static pressure and velocities of the mixture phase, and Y is the mass fraction of the gas phase.

The viscosity of the mixture phase μ, which is need for the estimation of the stress tensor τ in Eqs. (1), is estimated as follows [6];

$$\mu=(1-\alpha)(1+2.5\alpha)\mu_l+\alpha\mu_g \quad , \tag{2}$$

where α is the volume fraction of the gas phase (void fraction), and subscripts g and l denote the gas and liquid phases.

The governing equations Eqs.(1) are closed by the equation of state of the locally homogeneous two-phase medium. The equation of state is derived as follows by a linear combination of the mass of liquid phase with gas phase, where the liquid phase is expressed by Tammam type equation, which is compressible equation, and the gas phase is considered to be an ideal-gas:

$$\rho=\frac{p(p+p_c)}{K_l(1-Y)p(T+T_c)+R_gY(p+p_c)T} \quad , \tag{3}$$

where K_l is the liquid constant, R_g is the gas constant, and p_c and T_c are the pressure and temperature constants of the liquid.

The $\dot{m}$ in source term **S** of Eq. (1) is phase change speed, which is derived from the Hertz-Knudsen-Langumiur's equation for the present locally homogeneous medium as follows,

$$\dot{m}=\dot{m}^{+}=C_eA\alpha(1-\alpha)\left(\frac{\rho_l}{\rho_g}\right)\frac{p_v^*(T)-p}{\sqrt{2\pi RT}} \qquad \left(p<p_v^*(T)\right) \quad , \quad [\mathrm{kg/m^3s}] \tag{4}$$

$$\dot{m}=\dot{m}^{-}=C_cA\alpha(1-\alpha)\frac{p_v^*(T)-p}{\sqrt{2\pi RT}} \qquad \left(p>p_v^*(T)\right) \quad ,$$

$$A=C_a\alpha^{-\frac{1}{3}}(1-\alpha)^{-\frac{1}{3}} \quad ,$$

where $\dot{m}^{+}$ and $\dot{m}^{-}$ indicate evaporation and condensation respectively. The A is pseudo gas-liquid interface rate of the homogeneous gas-liquid medium, C_a is a constant for gas-liquid interface ratio, C_e and C_c are constants for evaporation and condensation. In the present study, the constants are set as $C_a{\cdot}C_e$ = $C_a{\cdot}C_o$= 0.01 for both water and liquid nitrogen calculations although it is still not fully adjusted. The saturated vapor pressure p_v*(T) of water and liquid nitrogen are both approximated by using experimental equation of saturated vapor pressure [7];

$$p_v(T)=p_0\exp\left(1-\frac{T_0}{T}\right)\left(a_1+(a_2+a_3T)\left(T-a_4{}^2\right)\right), \tag{5}$$

where, p_0 and T_0 are critical pressure and temperature for each fluid and a_1-a_4 are adjusting parameter.

The speed of sound of the two-phase medium derived from Eq. (3) has been verified experimentally based on the variation of void fraction [2]. Therefore, this numerical method is considered to be applicable to the reproduction of pressure wave propagation in a mixed flowfield of gas-liquid phases, which is important for numerical simulation of unsteady cavitation.

Simplified Thermodynamic Effect Model. In the present study, cavitating flowfield is calculated by above locally homogeneous and locally equilibrium model. On the other hand, thermodynamic effect with evaporation and condensation of cavitation is fundamentally non equilibrium phenomenon between liquid and gas phases. Therefore, calculation is performed in the present study by a simplified thermodynamic effect model, where local saturated vapor pressure of liquid phase changes with depending on the amount of heat transfer accompanied by evaporation and condensation.

The following thermodynamic model on cavitation is considered; when evaporation occurs, the amount of heat is considered to be deprived from liquid phase, which corresponds to increment of mass of gas phase. At that time, energy conservation equation is considered as follows.

$$\frac{\partial e_{neL}}{\partial t}+\frac{\partial\left((e_{neL}+p)u_j\right)}{\partial x_j}-\frac{\partial\left(\tau_{jk}u_k-\beta_j\right)}{\partial x_j}=\dot{q} \quad , \qquad \beta_j=-\kappa_l\frac{\partial T_{neL}}{\partial x_j} \quad , \tag{6}$$

where, subscript *neL* means liquid phase where thermal non-equilibrium assumption is taking account between gas and liquid phases. One has to be careful that the above liquid phase does not correspond to the liquid phase in the locally

homogeneous model. The heat transfer speed $\dot{q}$ in eq (6) is expressed by using $\dot{m}$ as follows;

$$\dot{q} = -\Delta\alpha\rho_g L/\Delta t = -\Delta Y\rho L/\Delta t = -\dot{m}L \quad [\mathrm{J/m^3 s}], \qquad (7)$$
$$L = \left(C_{p_g}T + h_{0g}\right) - \left(C_{p_l}T_{nonL} + h_{0l}\right),$$

where, L is latent heat which is difference of enthalpy between gas and liquid phase, and the enthalpy is evaluated by considering that isobaric specific heat capacity C_p is assumed constant. The T_{neL} is calculated from following equation about total energy of the non-equilibrium liquid phase.

$$e_{neL} = \rho\left\{C_{pl}T_{neL} + h_{0l} + \frac{\mathbf{u}^2}{2}\right\} - p. \qquad (8)$$

By using the T_{neL}, local saturated pressure for the non-equilibrium liquid phase is calculated from Eq. (5). Then, the evaporation speed in Eq. (4) is modified as follows in the simplified thermodynamic effect model.

$$\dot{m}^+ = C_e A\alpha(1-\alpha)\left(\frac{\rho_l}{\rho_g}\right)\frac{p_v^*(T_{neL}) - p}{\sqrt{2\pi RT}} \quad \left(p < p_v^*(T_{neL})\right). \qquad (9)$$

Numerical Scheme. In the present numerical method, since the cavity surface which is a discontinuity in density is described as the gradient of void fraction, a numerical method for contact discontinuity problem in compressible fluid can be used. Then, the cavity profile is not restricted. At the same time, the thickness of the cavity surface depends on the resolution of the computational mesh. Therefore, this numerical method is considered to be applicable to the numerical analysis of a wide range of cavitation conditions, with the exception of incipient cavitation.In the present study, the governing equations of Eq. (1) are solved using the finite difference method. Since it is necessary to simulate stably the discontinuities of the large density jump at the gas-liquid interface in a cavitating flowfield, the TVD scheme is used in order to ensure the monotonicity of the solution. Specifically, the explicit TVD-MacCormack scheme [8] which has 2nd-order accuracy in time and space is used. No turbulence model is applied in the present study because, as of yet, there are no reliable turbulence models for unsteady cavitation in cryogenic fluid [9].

Computational Condition. Target flowfield of this study is a three-blade cyclic flat-plate cascade as shown in Fig. 1, which is the most simplified configuration of thee blade axial-flow pump, and where the cavitation unsteadiness that cannot be observed around a single hydrofoil can be reproduced. The solidity is C / h =2.0, the stagger angle is γ= 75º, and the bladethickness is zero. Upstream area is two chord lengths from the inlet boundary to the leading edge of the blade, and downstream is three chord lengths from the trailing edge to the outlet boundary. One cascade passage has 261x71 mesh points. A non-slip condition is assumed on the wall boundary of the blades, a cyclic boundary condition is imposed at every three cascade passages in order to reproduce the circumferential instabilities in a cascade, such as rotating cavitation. In the inlet boundary, constant conditions of flow angle, temperature, total pressure and void fraction are applied, where static pressure is extrapolated, and velocity is calculated from the condition of constant total pressure. In the condition of constant total pressure, variation of static pressure is permitted and artificial reflection of static pressure is absorbed. In the outlet boundary, a constant static pressure condition is applied, and velocity, temperature and density are extrapolated.

The two kinds of temperature are selected for each fluid; 290 K and 360 K in water and 77.64 K and 88.64 K in liquid nitrogen, in order to compare the thermodynamic effect between fluids or temperatures in each fluid. The inflow velocity is approximately U_{in} = 12 m/s in all case. Then the non-dimensional thermodynamic parameter Σ^* derived by Franc [10], which is shown in Eq. (8), is estimated as shown in Table 1 for each temperature of water and liquid nitrogen under the condition of saturated pressure in the present study.

$$\Sigma^* = \frac{\left(\rho_g L\right)^2}{\rho_l^2 C_{p_l} T\sqrt{a_l}}\sqrt{\frac{C}{U_{in}^3}} \quad . \qquad (8)$$

Where, a is thermal diffusivity. According to the order of the value of Σ^* as shown in Table 1, thermodynamic effect on cavitation is considered to increase, and the development of cavitation will be suppressed.

Table 1 Thermodynamic parameter Σ^* at the present temperatures in each fluid under the condition of saturated

	Water		Liquid Nitrogen	
T	290K	360K	77.64K	88.64K
Σ^*	0.000658	0.314	7.79	46.2
Re	1.1×10^6	3.7×10^6	6.5×10^6	8.1×10^6

The inflow angle is selected α_{in} =7º, at which occurrence of several kinds of cavitation instabilities was observed in the previous numerical study of same cascade arrangement in room temperature water 293 K [3]. Computation is executed for several cavitation numbers σ, where σ is controlled by upstream static pressure that changes depending on static pressure in outlet boundary and the head performance of the cascade. Cavitation number σ, flow rate coefficient ϕ, and static pressure coefficient ψ are estimated as follows:

$$\text{Cavitation number:} \quad \sigma = \frac{p_{in} - p_v}{1/2\rho_{in}U_{in}^2} \quad , \qquad (9)$$

$$\text{Flow rate coefficient:} \quad \phi = U_a/U_t \quad , \qquad (10)$$

$$\text{Static pressure constant:} \quad \psi = \frac{p_{out} - p_{in}}{\rho_{in}U_t^2} \quad , \qquad (11)$$

where U_t and U_a are the circumferential and axial velocities, respectively, of U_{in}. Here σ and ψ are calculated from time averaged computational results for each case. The angles of attack α_{in} = 7 º corresponds to ϕ = 0.141.

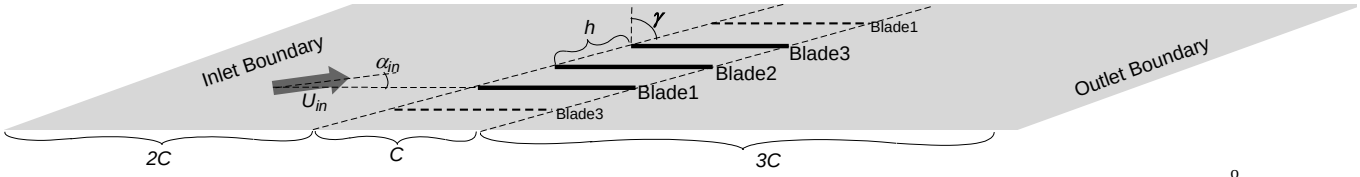

Fig.1 Schematic diagram of the three-blade cyclic flat-plate cascade of the present study (C/h = 2.0, γ=75°)

RESULTS AND DISCUSSIONS

Unsteady Cavitation in Water. At first, the typical flowfields of unsteady cavitation are compared between room temperature water and hot water under the condition of same cavity volume. Also, the both cases are in a condition of after head break down. Figure 2 shows time evolutions of aspect of flowfield at room temperature water (290K), which is composed of distributions of (a) void fraction, (b) evaporation speed, (c) condensation speed and (d) non-equilibrium temperature T_{neL}, which does not corresponds to temperature of flowfield. In void fraction distribution, it is shown that sheet cavity occurs and breaks in suction side of blade and cloud cavity is released downstream. The evaporation area is converged cavity surface which is extends from leading edge of blade when the sheet cavity is developing. Condensation area is found upstream and downstream of cloud cavity at the time of that cloud cavity is just released and the cloud cavity is still inside the cascade. When the cloud cavity moves downstream of the cascade, condensation area spreads inside the cloud cavity region. By affected the move of latent heat with the evaporation and condensation, which is expressed by right hand side term in Eq. (6), reference temperature of non-equilibrium liquid phase increases or decreases in the flowfield as shown in Fig.2 (d). The point we should notice is that the reference temperature does not correspond quantitatively to the local equilibrium temperature of the gas-liquid homogeneous medium, it corresponds to liquid temperature flowing with the homogeneous medium whose heat is deprived or provided with evaporation or condensation of the homogeneous medium and it is used just for estimation of saturated vapor pressure. The low temperature region distributes consistently in the sheet cavity, it is not only on the cavity surface but also inside the cavity. On the other hand, distribution of high temperature region roughly corresponds to condensation regions which are inside or around cloud cavity. It means that decrease in temperature is yielded by adiabatic expansion, and it is dominative in the cavitating flowfield compared to heat deprivation by evaporation. Also, because the fluid whose heat is deprived away on the cavity surface moves inside the cavity by separation flow, heat is derived from inside the cavity to the cavity surface by heat conduction accompanied by the flow, it is considered there is effect of phase change in some degree on temperature distribution. The saturated pressure estimated by the reference temperature increases or decreases in same way of the temperature.

The time evolution of the aspect of cavitating flowfield in hot water (360K) is shown in Fig. 3 (a) to (d). Although the time averaged cavity volume is almost same with that in 290K, the aspect of cavitation in 360K is quite different from that in 290K. It can be seen that the void fraction decreases wholly in the flowfield and there is no evident break-off of sheet cavity. The sheet cavity develops longwise to downstream and has complex undulating profile which is accompanied by vortex flow. The disturbance is considered to increase in this flowfield compared to that in 290K. The cloud cavity composed of low void fraction is observed to shed in this case. At that time, evaporation region is widely and briefly distributed near the leading edge of the blade or around the bank region of the undulating sheet cavity. Also, the condensation area spreads to all cavity regions that is from leading edge to downstream of the cascade. The reference temperature for estimation of saturated pressure seems to complexly distribute in the flowfield, where increased and decreased temperature regions are scattered in the cavity region. The adiabatic expansion and contraction inside the cavity with vortex configuration is considered to appear in the temperature distribution. The difference between flowfields at 290K and 360K which is about the cavity profile or distribution of phase change region is observed also in the iso-thermal calculation, it means the complexity does not come from thermodynamic effect on cavitation. It is considered that the turbulence intensity increases in high freestream temperature because of increase of Reynolds number which is accompanied by decrease of viscosity although the freestream velocity is constant as shown in Table 1, and it becomes a cause of the complex profile of the cavity in hot water shown in Fig. 3.

(a)

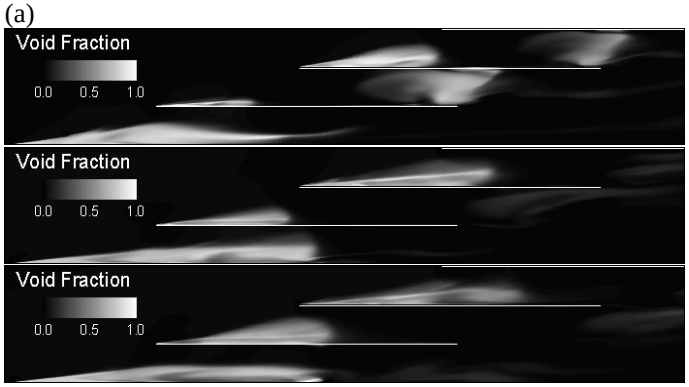

(b)

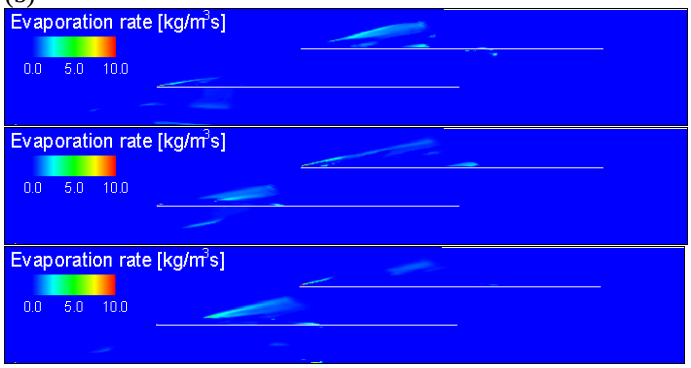

(c)

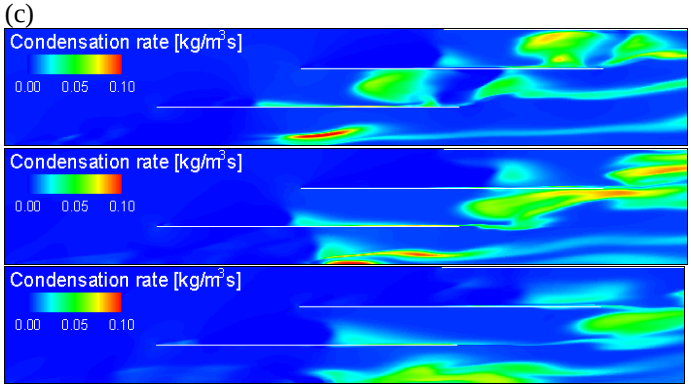

(d)

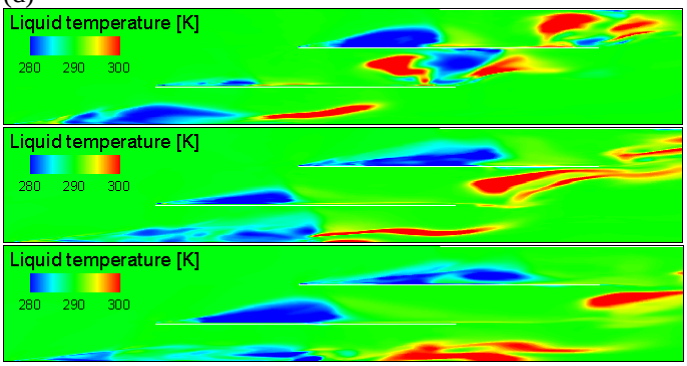

Fig. 2 Time evolution of distributions of (a) void fraction, (b) evaporation speed, (c) condensation speed, (d) reference temperature of liquid in water at 290K (σ = 0.0121, ψ = 0.159, ϕ = 0.141, time interval = 5ms)

(a)

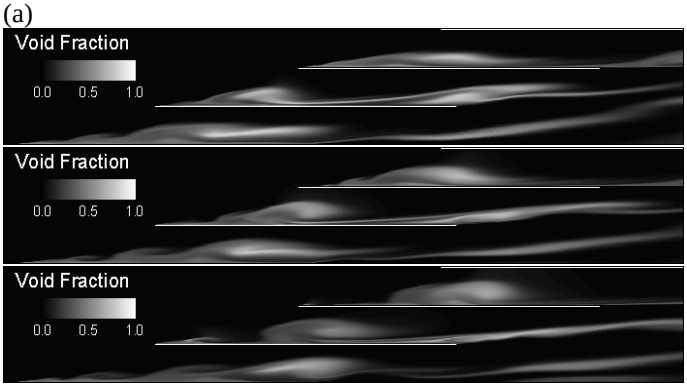

(b)

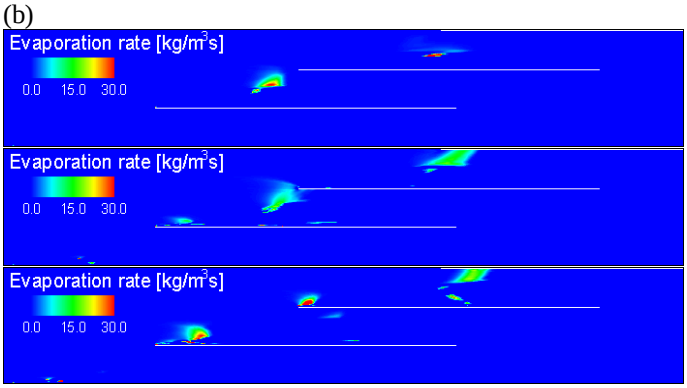

(c)

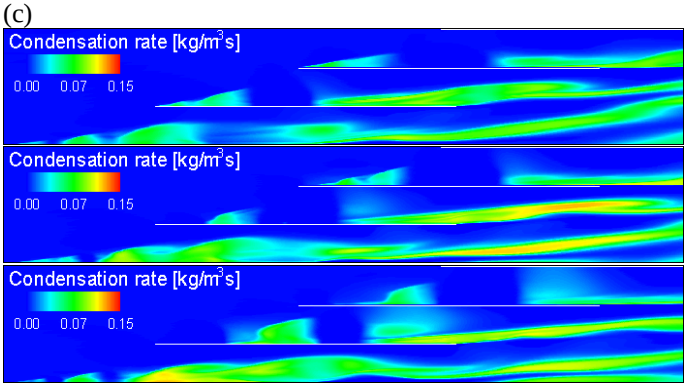

(d)

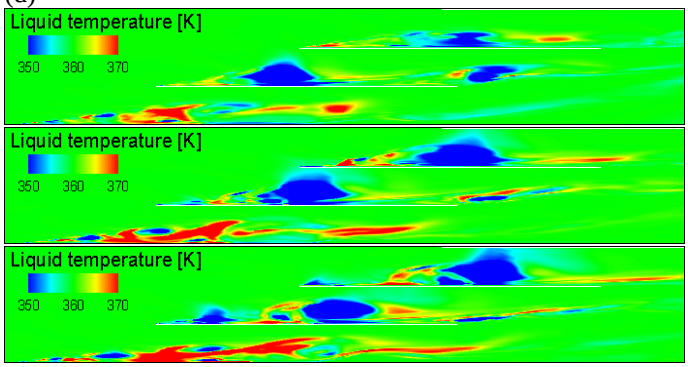

Fig.3 Time evolution of distributions of (a) void fraction, (b) evaporation speed, (c) condensation speed, (d) reference temperature of liquid in water at 360K (σ = 0.122, ψ = 0.144, ϕ = 0.141, time interval = 3 ms)

Unsteady Cavitation in Liquid Nitrogen. Next, the typical flowfield is compared between low and high temperature in liquid nitrogen and water. Figure 4 shows flowfields with unsteady cavitation at low temperature 77.64 K. The aspect of cavity Fig.4 (a) is almost same as that in hot water, where void fraction is low in whole flowfield and the profile of the cavity profile is undulating. Evaporation area (Fig. 4 (b)) is scattered inside of the cavity, which is not near the leading edge of the blade but rear area inside the cavity. At that time, the value of evaporation rate is extremely higher than that in hot water. In the evaporation rate of the present model which is expressed by Eq. (9). Although the density ratio between liquid and gas (ρ_l/ρ_g) is small in liquid nitrogen compared with that in water, therefore, $p_v^*(T_{nel}) - p$ is considered to increase largely in this case. It means that local static pressure drastically decreases because vorticity in cavity increases or saturated vapor pressure increases by increase of local temperature because the condition is near the critical point. The condensation region spreads in the whole cavity region and the rate also slightly increases compared to that in hot water. In the non-equilibrium temperature of liquid in Fig.4 (d), increased and decreased temperature regions distribute as scattering that is in a similar way of hot water, but the decreased temperature region seems to become narrow compared with that in hot water.

The time evolution of cavitating flowfield at high temperature 88.64K is shown in Fig. 5 (a) to (d). The aspect of cavity profile is almost same as that in low temperature. Also distributions of evaporation and condensation regions are almost same way in low temperature, but the evaporation rate is decreases, although that is higher than that in hot water and room temperature water. The non-equilibrium temperature is expressed from -10K to + 10K in all cases of water and liquid nitrogen, it is shown that both raised and dropped temperature regions are suppressed in nitrogen at high temperature. Generally, it is known experimentally that the thermodynamic effect on cavitation in cryogenic fluid becomes prominent according to increase of freestream temperature because temperature inside the cavity more drops and the saturated pressure more decreases [11]. The dropping region of the temperature shown in Fig. 2 to 5 (d) seems to be suppressed according to increase of Σ^*, it shows inverse tendency to the

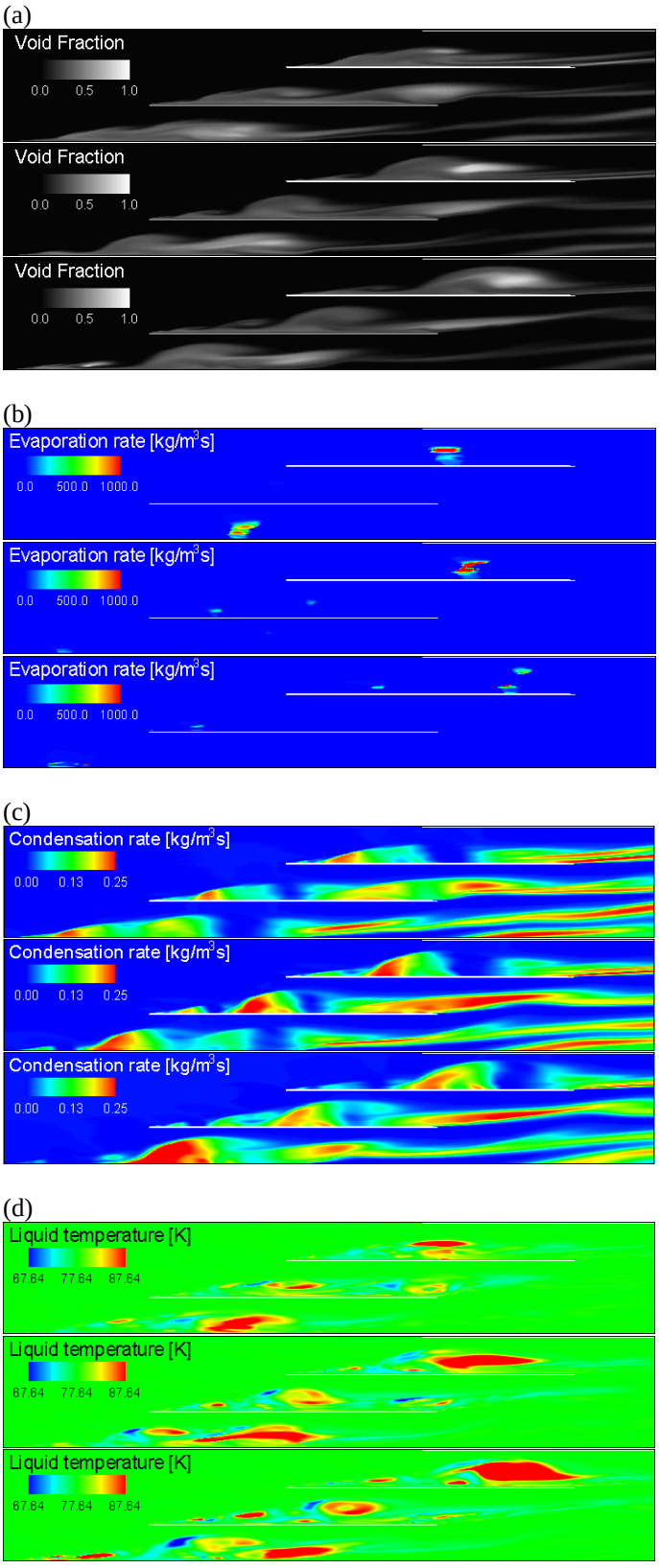

Fig. 4 Time evolution of distributions of (a) void fraction, (b) evaporation speed, (c) condensation speed, (d) reference temperature of liquid in liquid nitrogen at 77.64K (σ = 0.1221, ψ = 0.128, ϕ = 0.141, time interval = 3 ms)

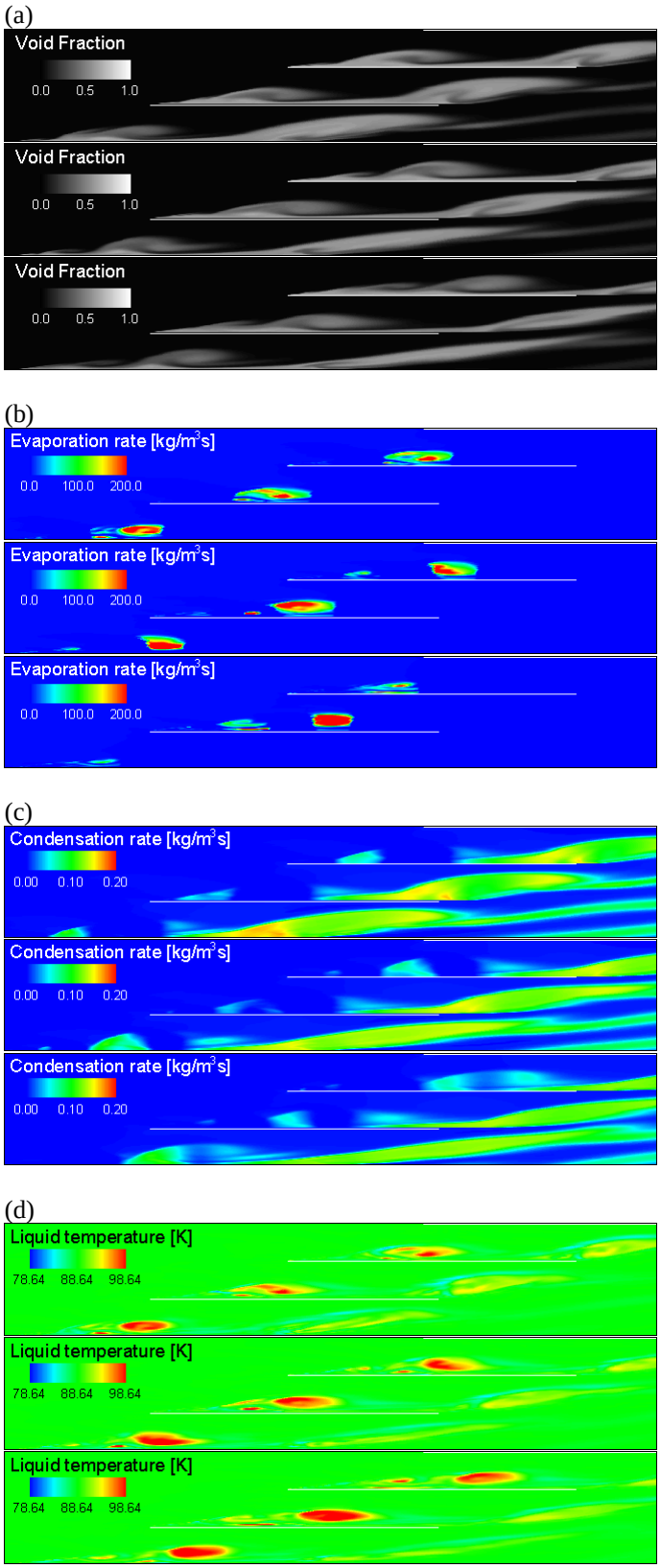

Fig. 5 Time evolution of distributions of (a) void fraction, (b) evaporation speed, (c) condensation speed, (d) reference temperature of liquid in liquid nitrogen at 88.64K (σ = 0.0034, ψ = 0.145, ϕ = 0.141, time interval = 3 ms)

experiment, although the present temperature cannot be compared with the experiment because the present temperature is not local temperature inside the cavity but the liquid temperature in simplified thermodynamic model.

Comparison of Cavity Volume and Head Performance. Time averaged cavity volumes in each cases of water and liquid nitrogen are shown in Fig. 6 with time averaged cascade head performance of each cases. The cavity volume is estimated by considering cavitation as a region where void fraction is over 1% and summing up the cell volume multiplied by the void fraction inside the cascade. Paying attention to the result of liquid nitrogen, which is shown by blue lines in Fig.6, cavity volume is becomes smaller at 88.64K compared to that at 77.64K when comparing at same cavitation number. Therefore, well known thermodynamic effect on cryogenic cavitation can be reproduced numerically in the present calculation. For reference, experimental result of inducer in liquid nitrogen at three temperatures obtained by authors [12] is shown in Fig.7. The qualitative tendency of cavity volume for temperature in the present numerical result in liquid nitrogen corresponds to the tendency of change of cavity length for temperature in the experiment. According to the suppression of development of cavity volume in the present study, drop point of head performance is seen to be delayed to lower cavitation number at 88.64compeared to 77.64K.

The results in water are shown by read marks and lines in Fig.6. In the result in water, in pseudo super cavitation condition where sheet cavity does not break off, which are the cases in lowest σ in each temperature, usual thermodynamic effect appears which mean that cavity volume becomes small at higher temperature. On the other hand, in transient cavitation with sheet cavity break-off as shown in Fig.2, cavity volume becomes small at lower temperature. It is inverse tendency of well known thermodynamic effect in cryogenic fluid. It is considerable to correspond to inverse thermodynamic effect which is experimentally observed in single hydrofoil in hot water [1]. Therefore, the inverse thermodynamic effect is considered to be yielded by concerning with unsteadiness of

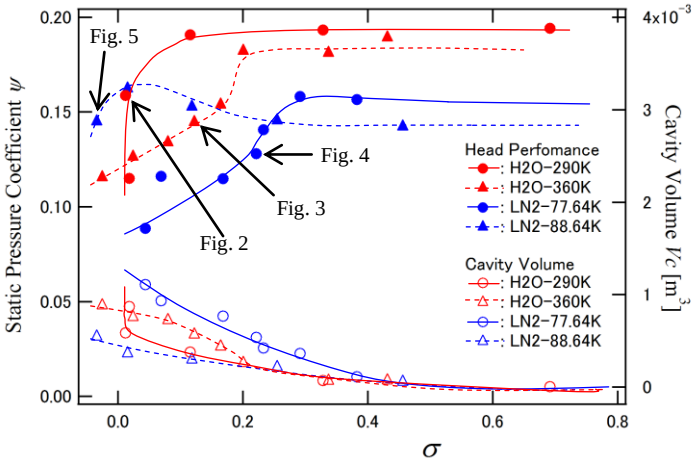

Fig.6 The change of time averaged head performance of the present three-blade cascade and the cavity volume at two temperatures in water and liquid nitrogen

cavitating flowfield especially in hot water. It may be given an explanation by considering increase of thermal diffusivity by turbulence, which decreases the thermodynamic parameter Σ^* in Eq. (8).

By comparing the results between water and liquid nitrogen, the cavity volume of liquid nitrogen at 77.64K is larger than that of water, although Σ^* in nitrogen at 77.64K is remarkably larger than that of water at 290K. It is hard to explain by only increase of thermal diffusivity, therefore, the present simplified thermodynamic model for locally homogeneous medium is considered to be not sufficient to reproduce whole thermodynamic effect in cavitating flowfield.

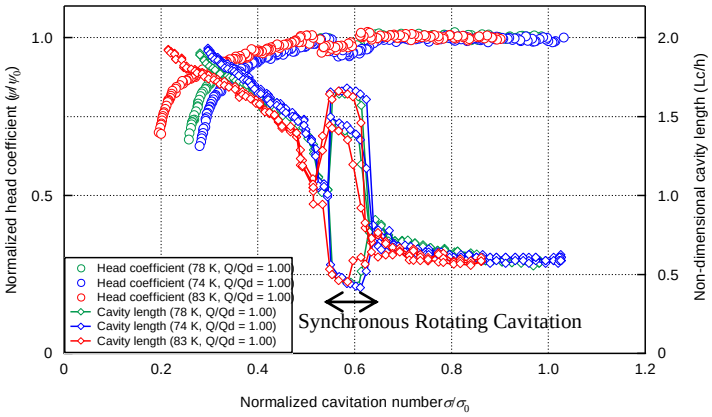

Fig.7 The change of time averaged head performance and cavity length in three-blade inducer with liquid nitrogen [12]

CONCLUSIONS

In the present study, unsteady cavitation is calculated in three-blade flat-plate cascade with working fluid of water and nitrogen, where two kinds of freestream temperatures are set for calculation of each fluid by using simplified thermodynamic effect model for locally homogeneous medium. The results are summarized as follows;

The difference of cavitating flowfields are reproduced numerically in water and liquid nitrogen at different freestream temperature. In room temperature water, where sheet cavity breaks off and cloud cavity sheds, the evaporation region is spread in the cavity surface when the sheet cavity is developing. On the other hand in hot water and liquid nitrogen, the cavity does not break off and the surface shows undulating profile by vortex flow, then evaporation is scatted around the cavity.

The thermodynamic effect on cavitation in liquid nitrogen is investigated by comparing the cavity volumes. Then, well known thermodynamic effect on cryogenic cavitation can be reproduced numerically in the present calculation, which is that development of cavity is suppressed according to increase of freestream temperature.

The inverse thermodynamic effect, which is experimentally observed in single hydrofoil in water, is reproduced under the condition of unsteady cavitation in the present study in water. Also, usual thermodynamic effect is shown in pseudo super-cavitation condition in water, therefore,

the inverse effect is considered to be yielded by unsteadiness and the turbulence of the cavitating flowfield.

By comparing the results of cavity volumes between water and liquid nitrogen, that of liquid nitrogen at lower temperature is larger than that of water, the result does not correspond to the magnitude relation of thermodynamic parameter Σ^*. Therefore, the present simplified thermodynamic model for locally homogeneous medium is necessary to be improved in order to reproduce whole thermodynamic effect in cavitating flowfield in various fluid.

REFERENCES

[1]Cervone, A., et.al., 2006, Journal of Fluids Engineering, Trans. ASME, Vol. 128, pp. 326-331.

[2] Iga, Y., Nohmi, M., Goto, A., Shin, B. R., and Ikohagi, T., 2003, "Numerical Study of Sheet Cavitation Break-off Phenomenon on a Cascade Hydrofoil", Journal of Fluids Engineering, Trans. ASME, Vol. 125-4, pp.643-651.

[3] Iga, Y., Nohmi, M., Goto, A., and Ikohagi, T., 2004, "Numerical Analysis of Cavitation Instabilities Arising in The Three-Blade Cascade", Journal of Fluids Engineering, Trans. ASME Vol. 126-3, pp. 419-429.

[4] Iga, Y., Hiranuma, Y. Yoshida, T., Ikohagi. T., 2008,"Numerical Analysis of Cavitation Instabilities and the Suppression in Cascade", Journal of Environment and Engineering, Vol.3-No.2, pp.240-249.

[5]Yoshinori Saito, Rieko Takami, Ichiro Nakamori, Toshiaki Ikohagi, 2007, "Numerical analysis of unsteady behavior of cloud cavitation around a NACA0015 foil", Comput Mech40:85-96.

[6] Beattie, D. R. H., Whally, P. B., 1982, "A Simple Two-Phase Frictional Pressure Drop Calculation Method", Int.. J. Multiphase Flow, Vol. 8, No. 1, pp. 83-87.

[7]Sugawara S, 1932, "New steam tables. Jpn Soc Mech Eng36(186):999-1004(in Japanese).

[8] Yee, H. C., 1987, "Upwind and Symmetric Shock-Capturing Schemes,"NASA-TM, 89464.

[9]Ashvin hosangadi, Vineet Ahuja, 2005, "Numerical Study of Cavitation in Cryogenic Fluids", Jounal of Fluids Engineering, Vol.127, pp 267-281.

[10]Franc J. P., Rebattet C., and Coulon A., 2004, "An Experimental Investigation of Thermal Effects in a Cavitating Inducer", J.Fluids Eng., 126, pp.716-723.

[11] Hord, J., 1973, " Cavitation in Liquid Crygens II-Hydrofoil", NASA CR-2156.

[12] Yoshida, Y., Sasao, Y., Okita, K., Hasegawa S., Shimagaki, M., Ikohagi, T., "Influence of Thermodynamic Effect on Synchronous Rotating Cavitation", Journal of Fluids Engineering, Trans. ASME Vol. 129, pp. 871-876.